Electronic Supplementary Information (ESI) for

Syntheses, Characterizations and Functions of Cationic Polyethers with Imidazolium-Based Ionic Liquid Moieties

Shigetaka Hayano, [a] Keisuke Ota, [a] and Hoang The Ban [a, b]*

[a] Zeon Corporation R&D Center, 1-2-1 Yako, Kawasaki-ward, Kawasaki-city, Kanagawa-pref., 210-9507, Japan

[b] Present address: Saigon Hi-Tech Park Incubation Center, K1-G3, D1 Road, Dist. 9, HCMC, Vietnam:

* Author for correspondence: e-mail: S.Hayano@zeon.co.jp

Fig. S1. Full scaled ^{1}H NMR (a) and ^{13}C NMR (b) spectra of poly(ECH-MeIm$^+$Cl$^-$) ($M_{n(calc)}$ = 18 900, DP = 108) obtaining from poly(ECH) (M_n = 10 000, M_w/M_n = 1.13, DP = 108; Table S1, run 7) (recorded in DMSO-d_6 at 27 °C).

Fig. S2. Full scaled ^{1}H NMR (a) and ^{13}C NMR (b) spectra of poly(ECH-MeIm$^+$TFSI$^-$) ($M_{n(calc)}$ = 45 400, DP = 108) obtaining from poly(ECH-MeIm$^+$Cl$^-$) stated in Fig. S1 (recorded in DMSO-d_6 at 27 °C).

Fig. S3. Full scaled ^{1}H NMR (a) and ^{13}C NMR (b) spectra of poly(ECH-MeIm$^+$BF$_4^-$) ($M_{n(calc)}$ = 24 500, DP = 108) obtaining from poly(ECH-MeIm$^+$Cl$^-$) stated in Fig. S1 (recorded in DMSO-d_6 at 27 °C).

Fig. S4. ^{1}H NMR spectra of ECH (top) and of an equimolar mixture of ECH and Et$_3$Al (bottom) (recorded in CDCl$_3$ at 27 °C).

Scheme S1. Plausible mechanism of coordination anionic polymerization of epoxide such as ethylene oxide by Al-based catalyst.

Scheme S2. Proposed mechanism of the present living anionic polymerization system for ECH.

Fig. S5. Effect of [ECH]/[*n*-Bu$_4$NBr] on molecular weight of poly(ECH) obtained from *n*-Bu$_4$NBr–Et$_3$Al (Table S1, run 5-9). (In the case of run 9, [ECH] × polymer yield/[*n*-Bu$_4$NBr] × 100 = 350 was used instead of [ECH]/[*n*-Bu$_4$NBr]).

Fig. S6. GPC chromatograms of multistage polymerization of ECH by *n*-Bu$_4$NBr–Et$_3$Al (1:1.2) (polymerized in toluene at 0 °C for 5h for the 1st stage polymerization (blue line), and polymerized in toluene at r.t. for 12h for the 2nd stage polymerization (red line); $[\text{ECH}]_o$ = 20 wt %, $[\text{ECH}]_{added}/[\text{ECH}]_o/[n\text{-Bu}_4\text{NBr}]$ = 150/50/1, 1.0 equivalent of Et$_3$Al was further added at the beginning of the 2nd stage polymerization) (eluent: THF).

Fig. S7. GPC chromatograms of poly(ECH)s synthesized by (a) *n*-Bu$_4$NBr–Et$_3$Al (1:1.2) (Table S1, run 7) and by (b) *n*-Bu$_4$NBr–*i*-Bu$_3$Al (1:1.2) (Table S1, run 11) (eluent: THF).

Fig. S8. Effect of reaction solvents on quaternization of poly(ECH) (M_n = 1 200, M_w/M_n = 1.22; Table S1, run 5)) by 1-methylimidazole (reacted at 80 °C, [poly(ECH) repeating unit]:[1-methylimidazole] = 1:2 (mol/mol)).

Fig. S9. Selected ^{1}H NMR spectra of [EMIm$^+$][Cl$^-$], poly(ECH-MeIm$^+$Cl$^-$) in Fig. S1(a), poly(ECH-MeIm$^+$TFSI$^-$) in Fig. S2(a) and [EMIm$^+$][TFSI$^-$] (recorded in DMSO-d_6 at 27 °C).

Fig. S10. GPC chromatograms of poly(ECH-MeIm$^+$Cl$^-$)s ((a) $M_{n(calc)}$ = 1 900; DP = 11, (b) $M_{n(calc)}$ = 5 800; DP = 33, (c) $M_{n(calc)}$ = 16 200; DP = 92) obtained from poly(ECH)s of different MW ((a) M_n = 1 080; DP = 11, (b) M_n = 3 050; DP = 33, (c) M_n = 8 500; DP = 92) (eluent: 0.1M $NaNO_3$ aq)).

Fig. S11. Selected ^{1}H NMR spectra of poly(ECH-MeIm$^+$TFSI$^-$)s with varied MWs ((a) $M_{n(calc)}$ = 4 610; DP = 11, (b) $M_{n(calc)}$ = 13 830; DP = 33, (c) $M_{n(calc)}$ = 38 550; DP = 92) (bottom) prepared through anion exchange of poly(ECH-MeIm$^+$Cl$^-$)s with varied MWs (top) (poly(ECH-MeIm$^+$Cl$^-$)s: (a) $M_{n(calc)}$ = 1 900; DP = 11, (b) $M_{n(calc)}$ = 5 800; DP = 33, (c) $M_{n(calc)}$ = 16 200; DP = 92) obtained from different poly(ECH)s ((a) M_n = 1 080; DP = 11, (b) M_n = 3 050; DP = 33, (c) M_n = 8 500; DP = 92) (recorded in DMSO-d_6 at 27 °C).

Fig. S12. Nyquist plots of poly(ECH-MeIm$^+$Cl$^-$) ($M_{n(calc)}$ = 4 700; DP = 27) prepared from poly(ECH) (M_n = 2 500; DP = 27; Table S1, run 6) after being exposed to air having various humidity ((a)20%, (b)40%, (c)60%, (d)80% RH at 23 °C) for 24 h, of which results are summarized in Table 3.

Fig. S13. DSC thermograms (heating steps) of poly(ECH-MeIm$^+$Cl$^-$) ($M_{n(calc)}$ = 18 900, DP = 108), poly(ECH-MeIm$^+$TFSI$^-$) ($M_{n(calc)}$ = 45 400, DP = 108) and the equimolar mixture of the two (determined under N_2, 10 °C/min for each step).

Experimental Part

Living Anionic Polymerization of Epichlorohydrin.

Living anionic ring-opening polymerization of epichlorohydrin (ECH) has been investigated in toluene using tetraalkylammonium bromide−trialkylaluminum initiator systems (Table S1). *n*-Bu_4NBr−Et_3Al was employed as an initiator system at first. Neither *n*-Bu_4NBr nor Et_3Al alone promoted ECH polymerization. *n*-Bu_4NBr was insoluble in non-polar solvent such as toluene, however, it readily dissolved in toluene after mixing with equimolar Et_3Al to become almost homogeneous, suggesting formation of ate-complex. Expecting from Deffieux's results, *n*-Bu_4NBr−Et_3Al (1:1) did not promote polymerization.[29−,31] 0.2 Equivalent excess of Et_3Al with respect to *n*-Bu_4NBr was necessary and enough in order to obtain poly(ECH) with low molecular weight ($M_n < 15\ 000$, $M_w/M_n < 1.25$) within several hours at 0 °C. At the meantime, 1.5 equivalents of Et_3Al appeared suitable to produce poly(ECH) with higher molecular weight ($M_n > 15\ 000$). When more than two equivalents of Et_3Al were employed, polymerization proceeded vigorously to end in formation of polymer with broad MWD. From these results, it can be said that suitable Et_3Al/*n*-Bu_4NBr ratio should be carefully chosen in order for controlling MW and MWD, because an excess amount of alkylaluminum would be a key to induce ECH polymerization. In order to gain an insight of elementary reaction of the polymerization, we studied an interaction between ECH and Et_3Al next. Fig. S4 depicts selected ^{1}H NMR charts of ECH and ECH−Et_3Al (1:1). In the case of ECH−Et_3Al (1:1) mixture, signals of α-proton of ECH shifted to downfield, indicating decrease of electrondensity on α-carbon by coordination of oxygen atom of epoxy group to Et_3Al. To summarize, monomer activation mechanism of the present system might be very close to that of well-established coordination anionic polymerization system suggested by Vandenberg *et al*. (Scheme S1).[23] For better understanding, a plausible mechanism of the present polymerization system is illustrated in Scheme S2 with reference to the report by Deffieux *et al*.[29,30] As described in Scheme S2, an initiator is ammonium salt (e.g., *n*-Bu_4NBr), whereas organoaluminum (Et_3Al) plays a role of activator for both initiator and monomer. The initiation reaction is a nucleophilic addition of bromide anion to epoxy α-carbon. Therefore in this case all the poly(ECH) has a bromo group as an initiation end.

Livingness of the present polymerization system was verified based on the results stated in Table S1. Fig. S5 is a [initial monomer](g/L)/[initiator](mol/L) ($[M]_o/[I]$) plot for the polymerization of ECH by *n*-$Bu_4NBr-Et_3Al$ (all the polymerization data is stated in Table S1, run 5-8). It is worthy to note that M_n of the obtained poly(ECH)s increased in direct proportion to $[M]_o/[I]$ with keeping their narrow MWDs, strongly indicating its living nature. It is also clarified that initiation efficiency of *n*-$Bu_4NBr-Et_3Al$ was almost 100%. Livingness of the polymerization was also confirmed by multistage polymerization (Fig. S6).

Next, effect of polymerization temperature was studied briefly on the living polymerization of ECH by *n*-$Bu_4NBr-Et_3Al$ (1:1.2) initiator system. Polymerization of ECH was less controllable at room temperature or higher: M_w/M_n of the obtained polymer was sometimes around 1.5 and reproducibility of polymerization was low. In contrast, 0 °C appeared to be a suitable temperature for smooth living polymerization: it took 5 h to finish polymerization to provide poly(ECH) with narrow MWD ($M_w/M_n < 1.2$) with high reproducibility.

Further, effect of activator was investigated for *n*-Bu_4NBr–trialkylaluminum initiator systems. To our results, Et_3Al was verified to be the best for *n*-Bu_4NBr to control the ECH polymerization in a living manner. Me_3Al was also a suitable activator in terms of obtaining narrow MWD and controlled molecular weight, while reproducibility of the polymerization was relatively low. Polymerization became sluggish when *n*-Oc_3Al was employed. It was in contradiction to our expectation that the polymerization by *n*-Bu_4NBr–*i*-Bu_3Al proceeded vigorously at 0 °C and always levelled off to form poly(ECH) with broad MWD (Fig. S7). Similarly, *n*-Oc_4NBr–*i*-Bu_3Al reported by Deffieux was not suitable for ECH polymerization at mild condition. We have found that the control of the reaction temperature was crucial for the present living polymerization system. In the case of *n*-Bu_4NBr–*i*-Bu_3Al, the temperature of the reaction mixture elevated up to 30 °C within 3 minutes to lose its polymerization activity. It is proposed that *i*-Bu_3Al activates ammonium initiator excessively for the present polymerization condition. In contrast *i*-Bu_3Al–*n*-$alkyl_3Al$ works mildly at 0 °C.

Further, (*n*-alkyl)$_4$NBr as an initiator was varied for the present initiator systems. When Me_4NBr was employed, phase separation of the catalyst mixture was observed, indicating low solubility of Me_4NBr–Et_3Al in toluene. Predictably polymerization was irreproducible, but gave low MWD polymers. *n*-Oc_4NBr was found to be also useful as an initiator. As a conclusion, *n*-Bu_4NBr–Et_3Al (1:1.2) was proved to be the most useful initiator system to synthesize poly(ECH) with controllable MW and MWD quantitatively, and was employed for this study.

Table S1. Living Ring-Opening Anionic Polymerization of Epichlorohydrin (ECH) by Various Initiator Systems [a]

run	initiators	activators	N:Al mole ratio	$[ECH]_o/[I]$	polymn. temp.	polymer yield, %	M_n	M_w/M_n
1	*n*-Bu_4NBr	Et_3Al	1:0	11	22 °C		no polymer	
2	*n*-Bu_4NBr	Et_3Al	0:1	11	22 °C		no polymer	
3	*n*-Bu_4NBr	Et_3Al	1:1	11	22 °C		no polymer	
4	*n*-Bu_4NBr	Et_3Al	1:1.2	108	22 °C		irreproducible	
5	*n*-Bu_4NBr	Et_3Al	1:1.2	11	0 °C	100	1 200	1.22
6	*n*-Bu_4NBr	Et_3Al	1:1.2	27	0 °C	100	2 500	1.20
7	*n*-Bu_4NBr	Et_3Al	1:1.2	108	0 °C	99	10 000	1.13
8	*n*-Bu_4NBr	Et_3Al	1:1.5	216	0 °C	97	19 900	1.30
9	*n*-Bu_4NBr	Et_3Al	1:1.5	432	0 °C	81 [b]	32 200	1.16
10	*n*-Bu_4NBr	Me_3Al	1:1.2	11	0 °C	100	1 100	1.14
11	*n*-Bu_4NBr	*i*-Bu_3Al	1:1.2	108	0 °C	100	10 700	1.29
12	*n*-Bu_4NBr	*n*-Oc_3Al	1:1.5	432	0 °C	21 [b]	8 300	1.16
13	Me_4NBr	Et_3Al	1:1.2	11	0 °C	100	1 200	1.32
14	*n*-Oc_4NBr	Et_3Al	1:1.2	11	0 °C	100	1 100	1.24

[a] Polymerized in toluene for 5h; [ECH] = 20 wt %. [b] Polymerized for 12h

Fig. S1. Full scaled ^{1}H NMR (a) and ^{13}C NMR (b) spectra of poly(ECH-MeIm$^+$Cl$^-$) ($M_{n(calc)}$ = 18 900, DP = 108) obtained from poly(ECH) (M_n = 10 000, M_w/M_n = 1.13, DP = 108; Table S1, run 7) (recorded in DMSO-d_6 at 27 °C).

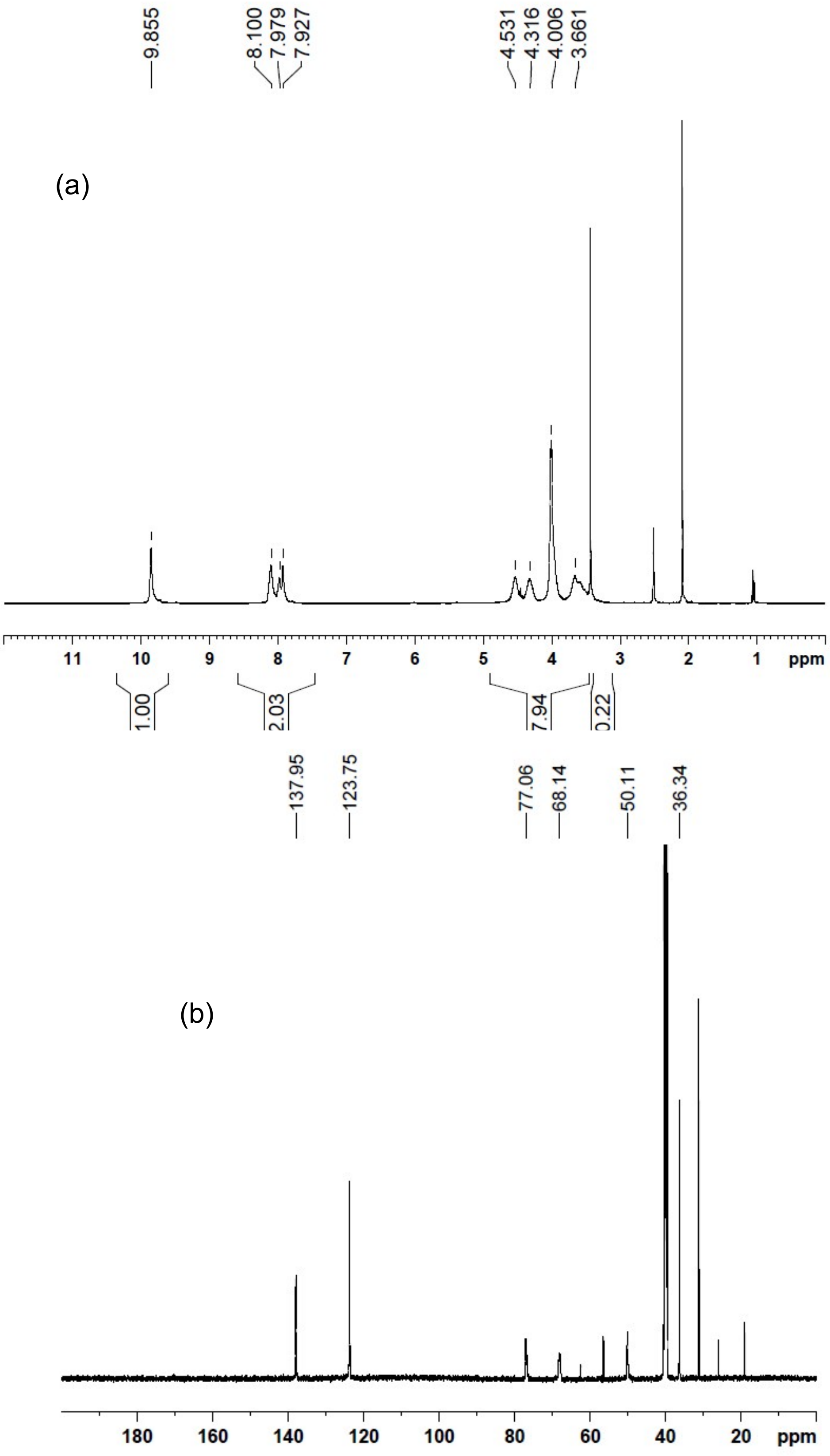

Fig. S2. Full scaled ^{1}H NMR (a) and ^{13}C NMR (b) spectra of poly(ECH-MeIm^{+}TFSI^{-}) ($M_{\text{n(calc)}}$ = 45 400, DP = 108) obtained from poly(ECH-MeIm^{+}Cl^{-}) stated in Fig. S1 (recorded in DMSO-d_6 at 27 °C).

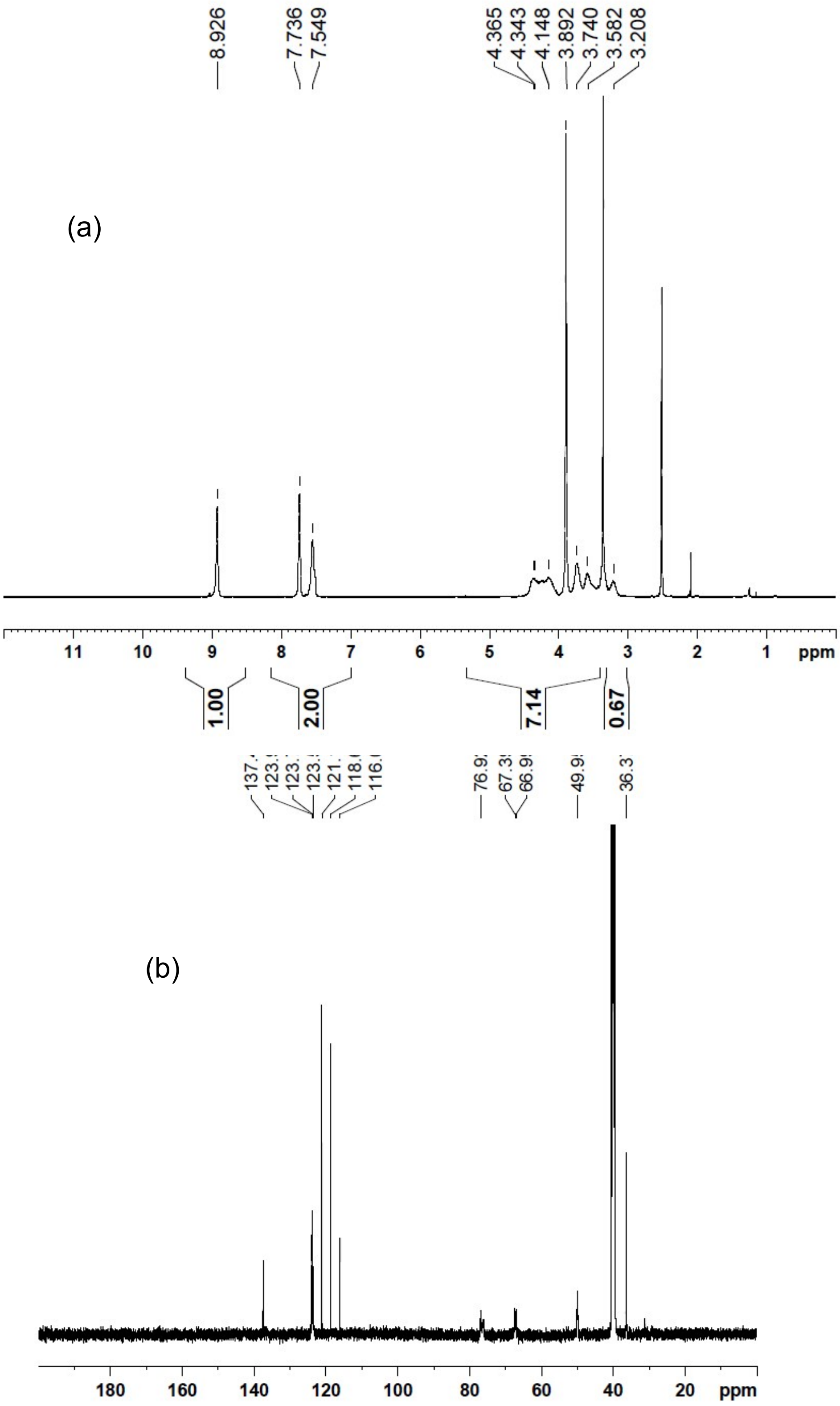

Fig. S3. Full scaled ^{1}H NMR (a) and ^{13}C NMR (b) spectra of poly(ECH-MeIm^{+}BF$_4^{-}$) ($M_{\mathrm{n(calc)}}$ = 24 500, DP = 108) obtained from poly(ECH-MeIm^{+}Cl^{-}) stated in Fig. S1 (recorded in DMSO-d_6 at 27 °C).

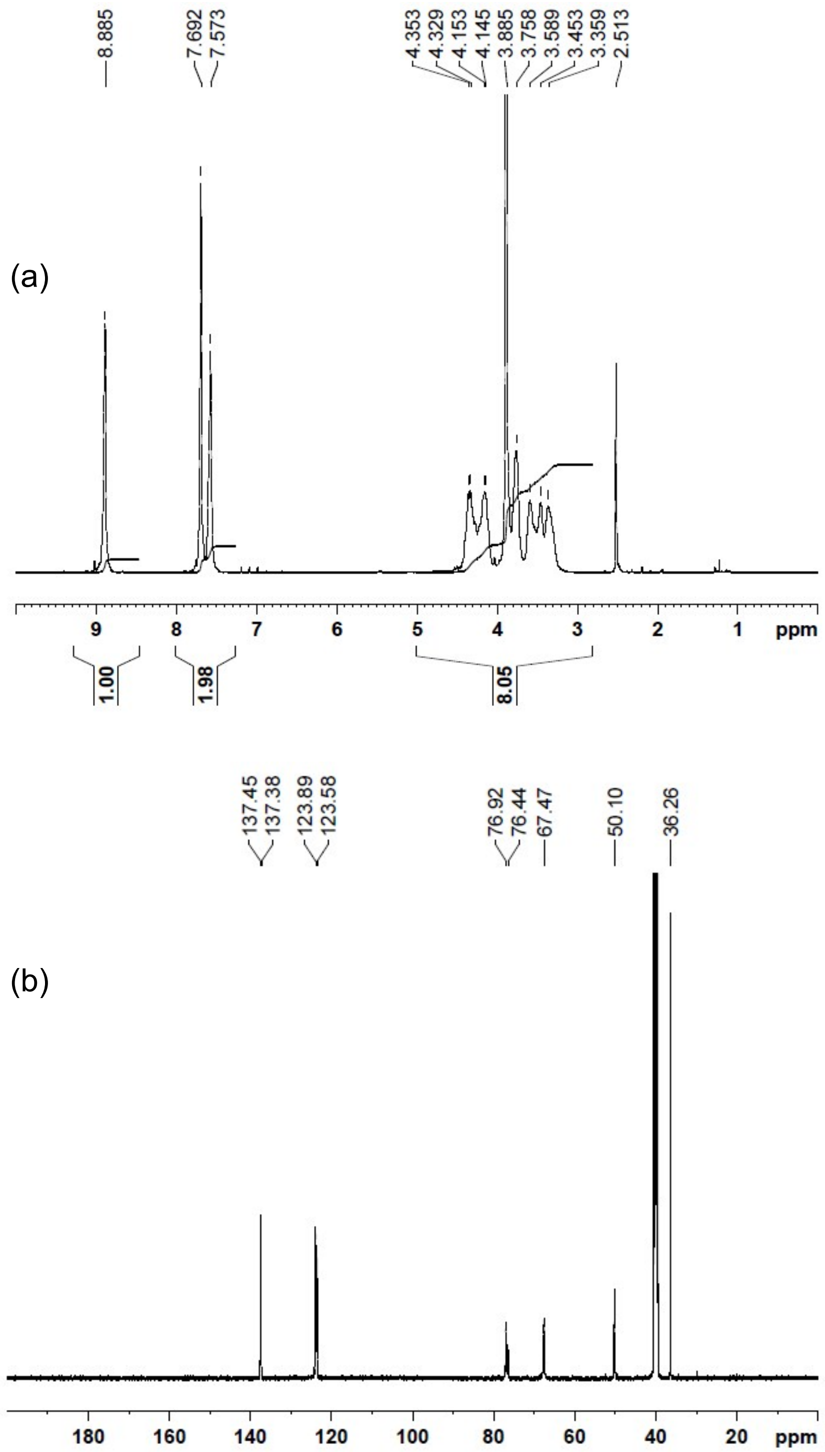

Fig. S4. ^{1}H NMR spectra of ECH (top) and of an equimolar mixture of ECH and Et_3Al (bottom) (recorded in $CDCl_3$ at 27 °C).

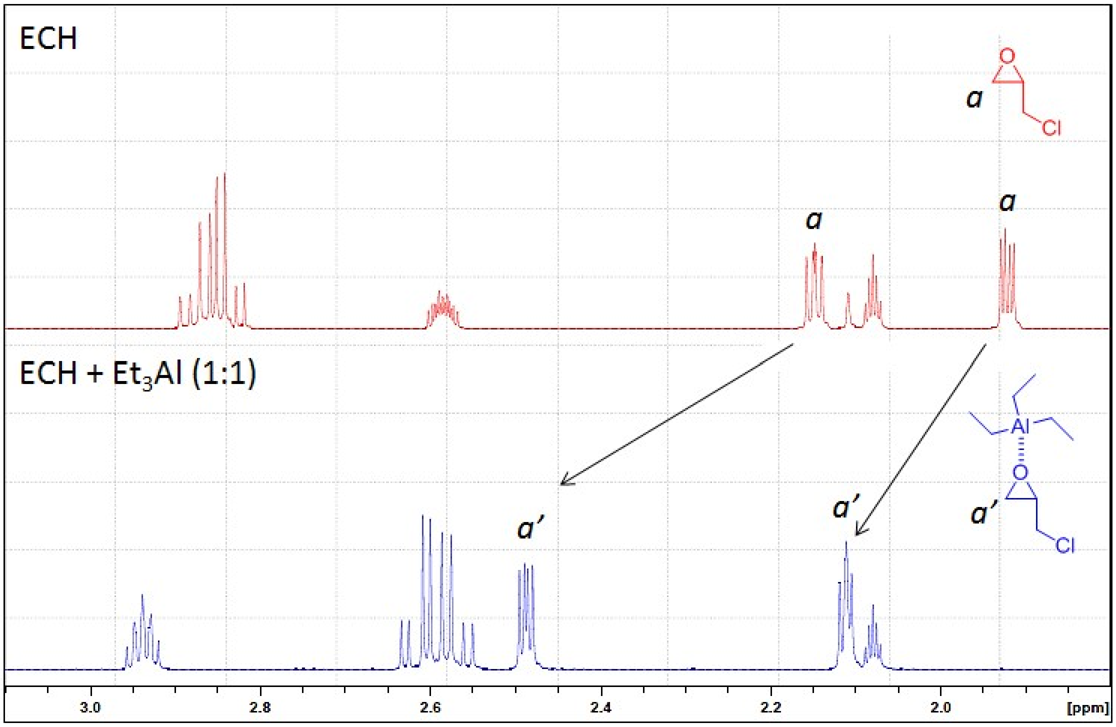

Scheme S1. Plausible mechanism of coordination anionic polymerization of epoxide such as ethylene oxide by Al-based catalyst.

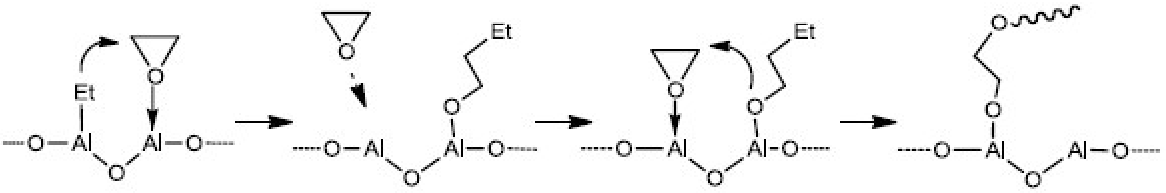

Scheme S2. Proposed mechanism of the present living anionic polymerization system for ECH.

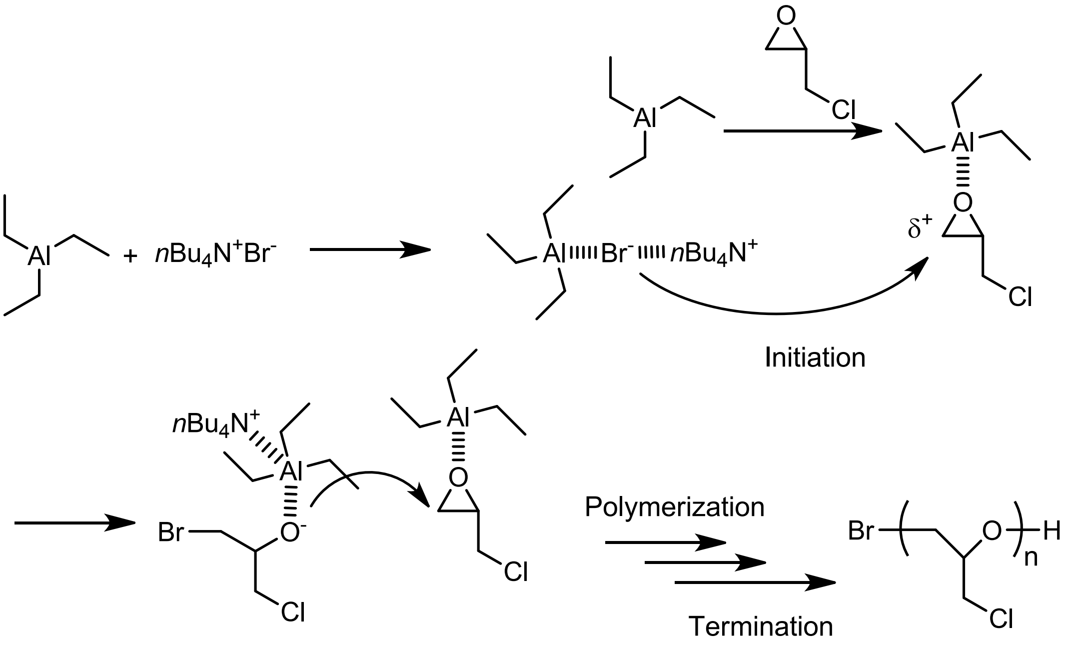

Fig. S5. Effect of [ECH]/[n-Bu_4NBr] on molecular weight of poly(ECH) obtained from n-Bu_4NBr–Et_3Al (Table S1, run 5-9). (In the case of run 9, [ECH] × polymer yield/[n-Bu_4NBr] × 100 = 350 was used instead of [ECH]/[n-Bu_4NBr]).

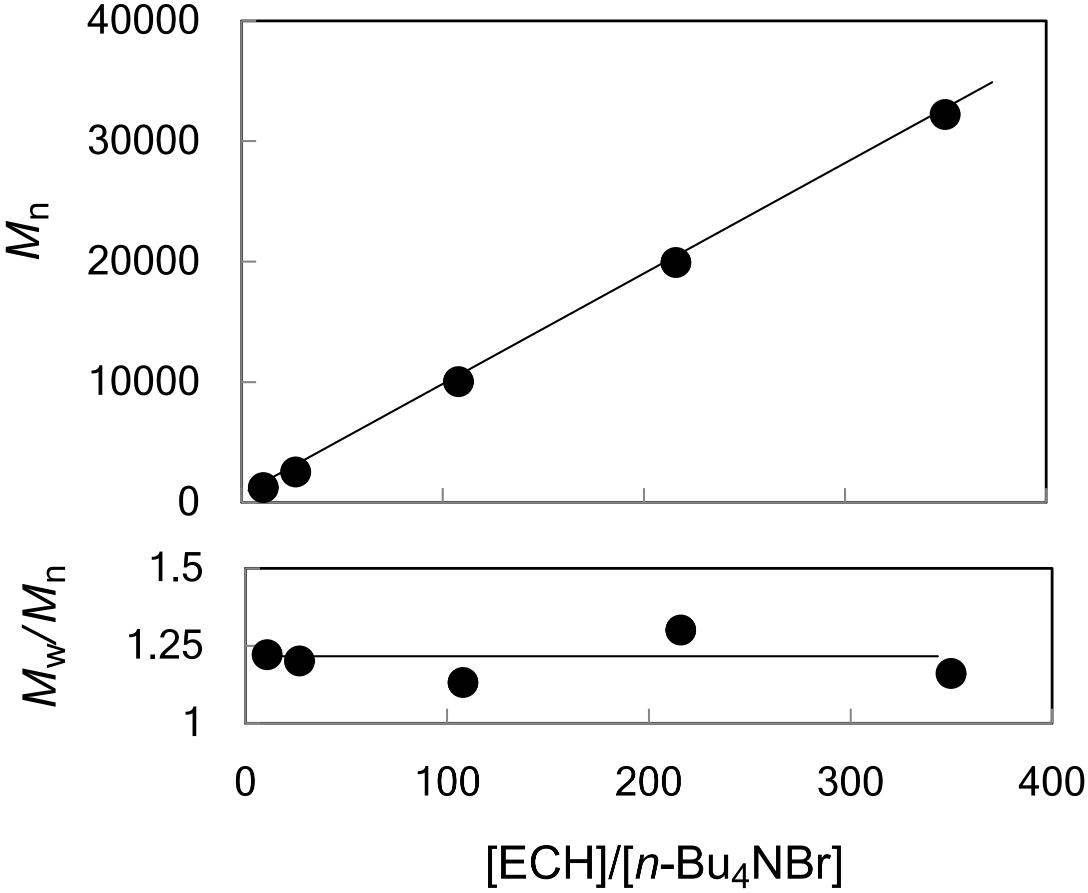

Fig. S6. GPC chromatograms of multistage polymerization of ECH by *n*-Bu$_4$NBr–Et$_3$Al (1:1.2) (polymerized in toluene at 0 °C for 5h for the 1st stage polymerization (blue line), and polymerized in toluene at r.t. for 12h for the 2nd stage polymerization (red line); $[\mathrm{ECH}]_o$ = 20 wt %, $[\mathrm{ECH}]_{\mathrm{added}}/[\mathrm{ECH}]_o/[n\text{-Bu}_4\mathrm{NBr}]$ = 150/50/1, 1.0 equivalent of Et$_3$Al was further added at the beginning of the 2nd stage polymerization) (eluent: THF).

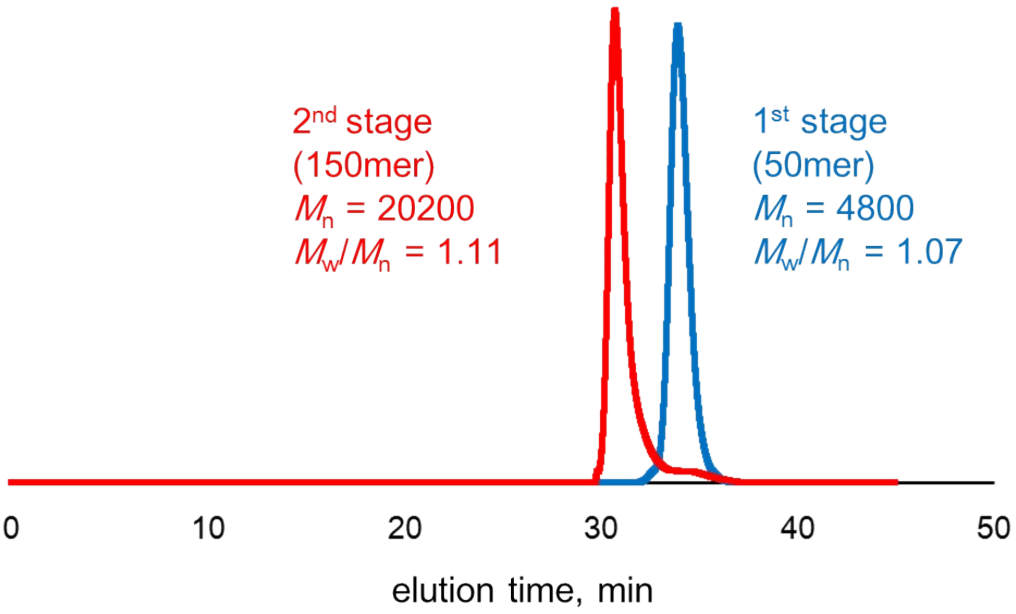

Fig. S7. GPC chromatograms of poly(ECH)s synthesized by (a) *n*-Bu$_4$NBr–Et$_3$Al (1:1.2) (Table S1, run 7) and by (b) *n*-Bu$_4$NBr–*i*-Bu$_3$Al (1:1.2) (Table S1, run 11) (eluent: THF).

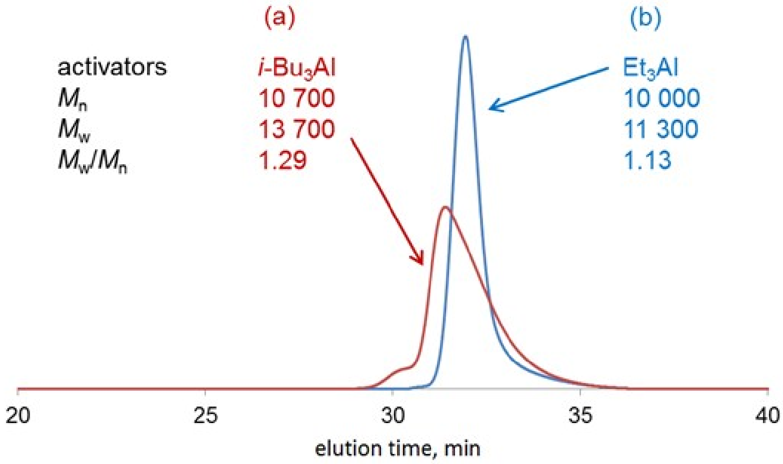

Fig. S8. Effect of reaction solvents on quaternization of poly(ECH) (M_n = 1 200, M_w/M_n = 1.22; Table S1, run 5)) by 1-methylimidazole (reacted at 80 °C, [poly(ECH) repeating unit]:[1-methylimidazole] = 1:2 (mol/mol)).

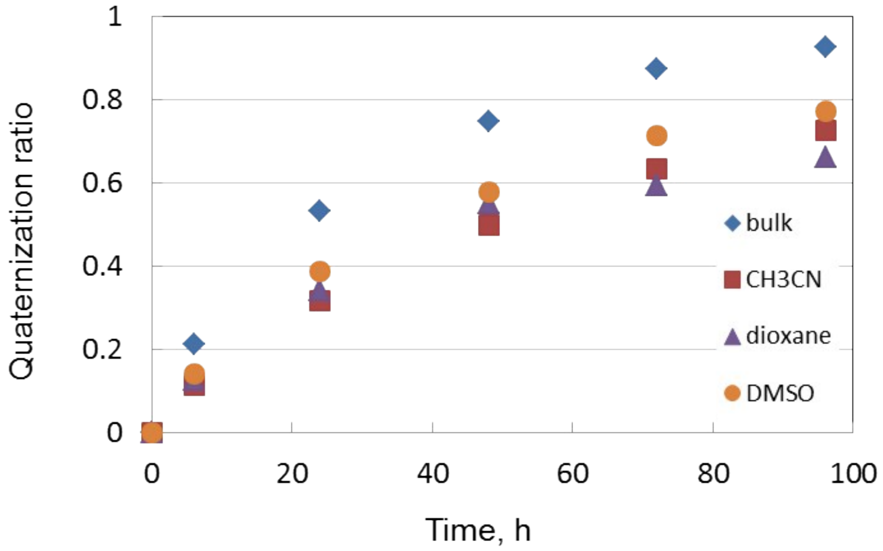

Fig. S9. Selected ^{1}H NMR spectra of [EMIm$^+$][Cl$^-$], poly(ECH-MeIm$^+$Cl$^-$) in Fig. S1(a), poly(ECH-MeIm$^+$TFSI$^-$) in Fig. S2(a) and [EMIm$^+$][TFSI$^-$] (recorded in DMSO-d_6 at 27 °C)

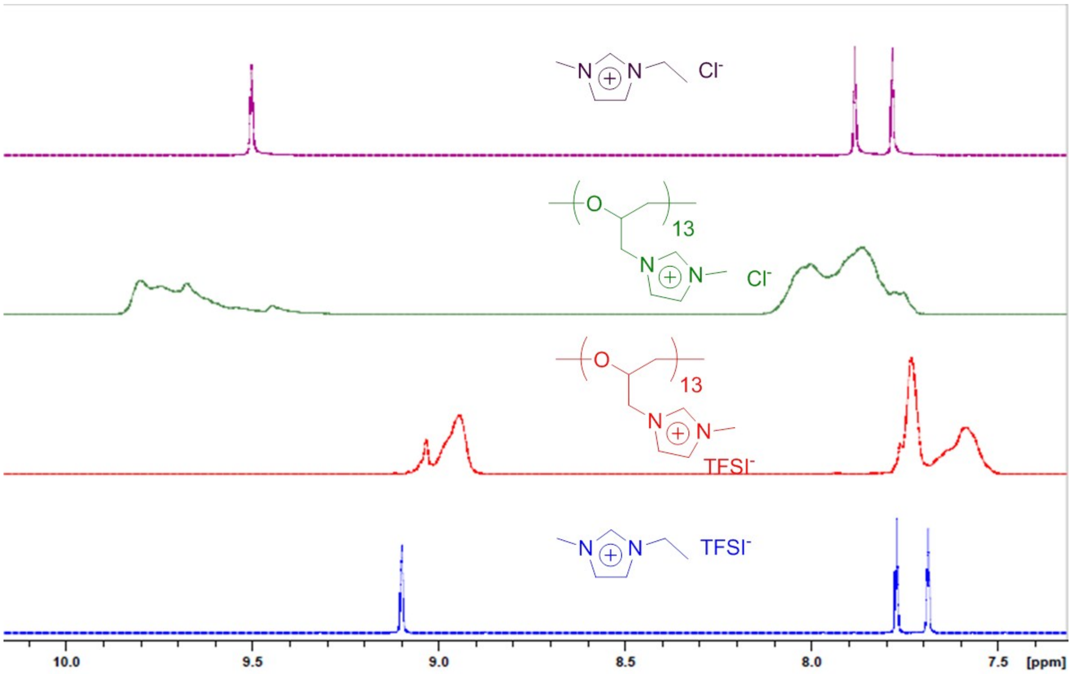

Fig. S10. GPC chromatograms of poly(ECH-MeIm$^+$Cl$^-$)s ((a) $M_{n(calc)}$ = 1 900; DP = 11, (b) $M_{n(calc)}$ = 5 800; DP = 33, (c) $M_{n(calc)}$ = 16 200; DP = 92) obtained from poly(ECH)s of different MW ((a) M_n = 1 080; DP = 11, (b) M_n = 3 050; DP = 33, (c) M_n = 8 500; DP = 92) (eluent: 0.1M $NaNO_3$ aq)).

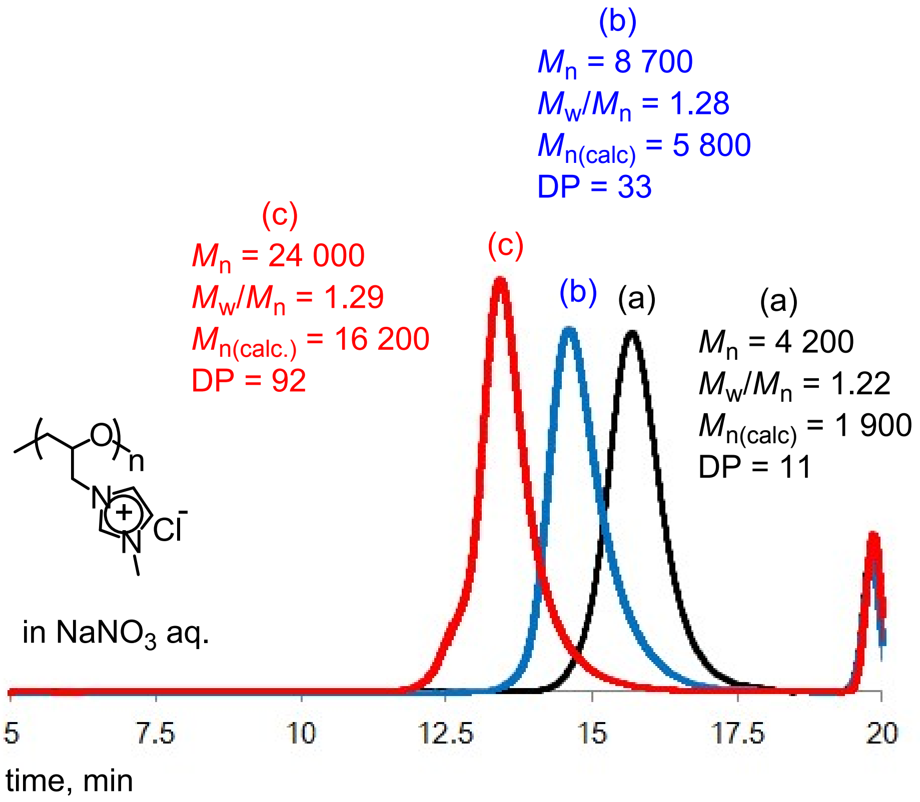

Fig. S11. Selected ^{1}H NMR spectra of poly(ECH-MeIm$^+$TFSI$^-$)s with varied MWs ((a) $M_{n(calc)}$ = 4 610; DP = 11, (b) $M_{n(calc)}$ = 13 830; DP = 33, (c) $M_{n(calc)}$ = 38 550; DP = 92) (bottom) prepared through anion exchange of poly(ECH-MeIm$^+$Cl$^-$)s with varied MWs (top) (poly(ECH-MeIm$^+$Cl$^-$)s: (a) $M_{n(calc)}$ = 1 900; DP = 11, (b) $M_{n(calc)}$ = 5 800; DP = 33, (c) $M_{n(calc)}$ = 16 200; DP = 92) obtained from different poly(ECH)s ((a) M_n = 1 080; DP = 11, (b) M_n = 3 050; DP = 33, (c) M_n = 8 500; DP = 92) (recorded in DMSO-d_6 at 27 °C).

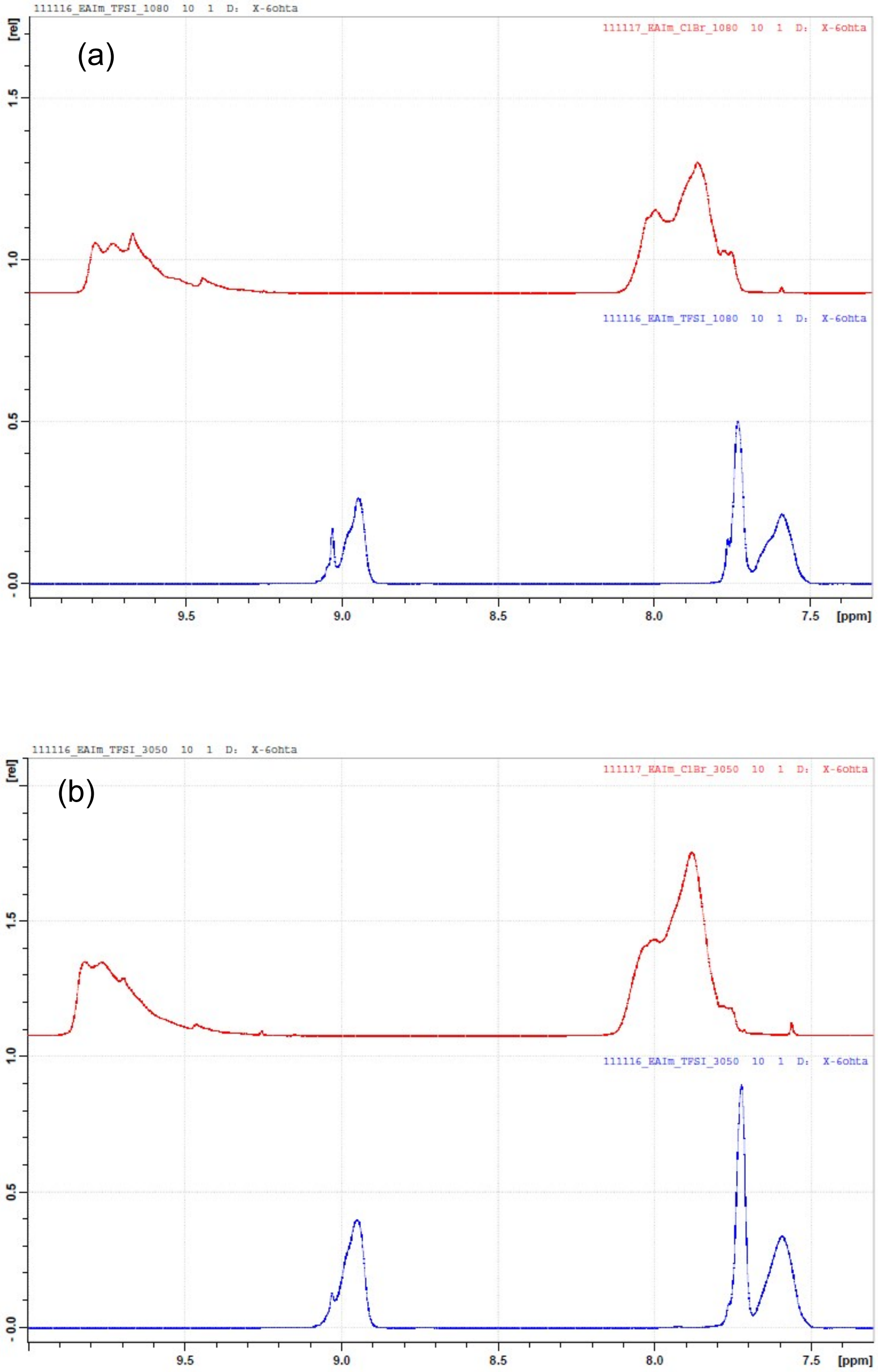

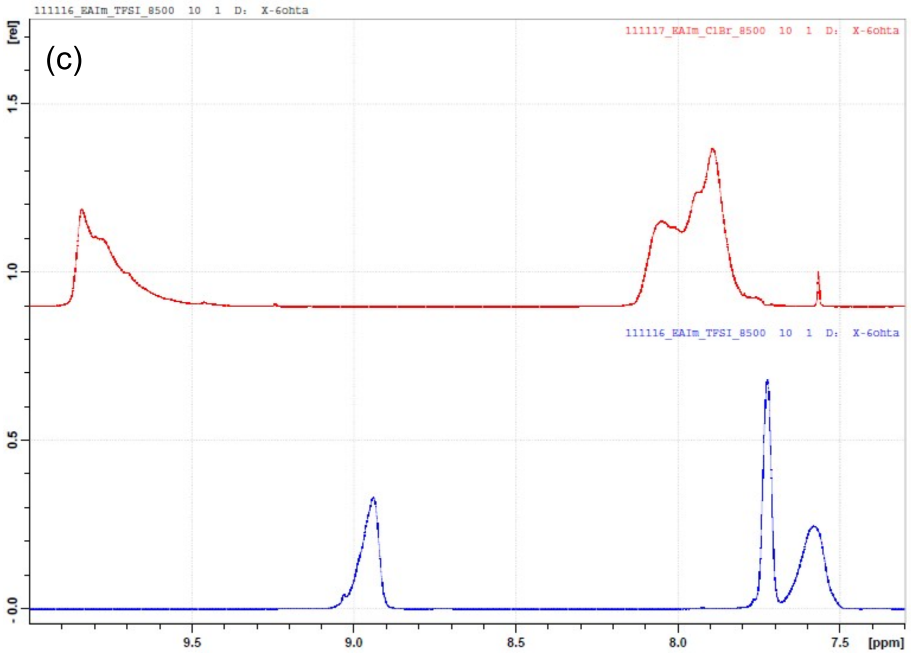
111116_EAIm_TFSI_8500 10 1 D: X-6ohta
(c)
111117_EAIm_ClBr_8500 10 1 D: X-6ohta
111116_EAIm_TFSI_8500 10 1 D: X-6ohta
[rel]
1.5
1.0
0.5
0.0
9.5
9.0
8.5
8.0
7.5
[ppm]

Fig. S12. Nyquist plots of poly(ECH-MeIm$^+$Cl$^-$) ($M_{n(calc)}$ = 4 700; DP = 27) prepared from poly(ECH) (M_n = 2 500; DP = 27; Table S1, run 6) after being exposed to air having various humidity ((a)20%, (b)40%, (c)60%, (d)80% RH at 23 °C) for 24 h, of which results are summarized in Table 3.

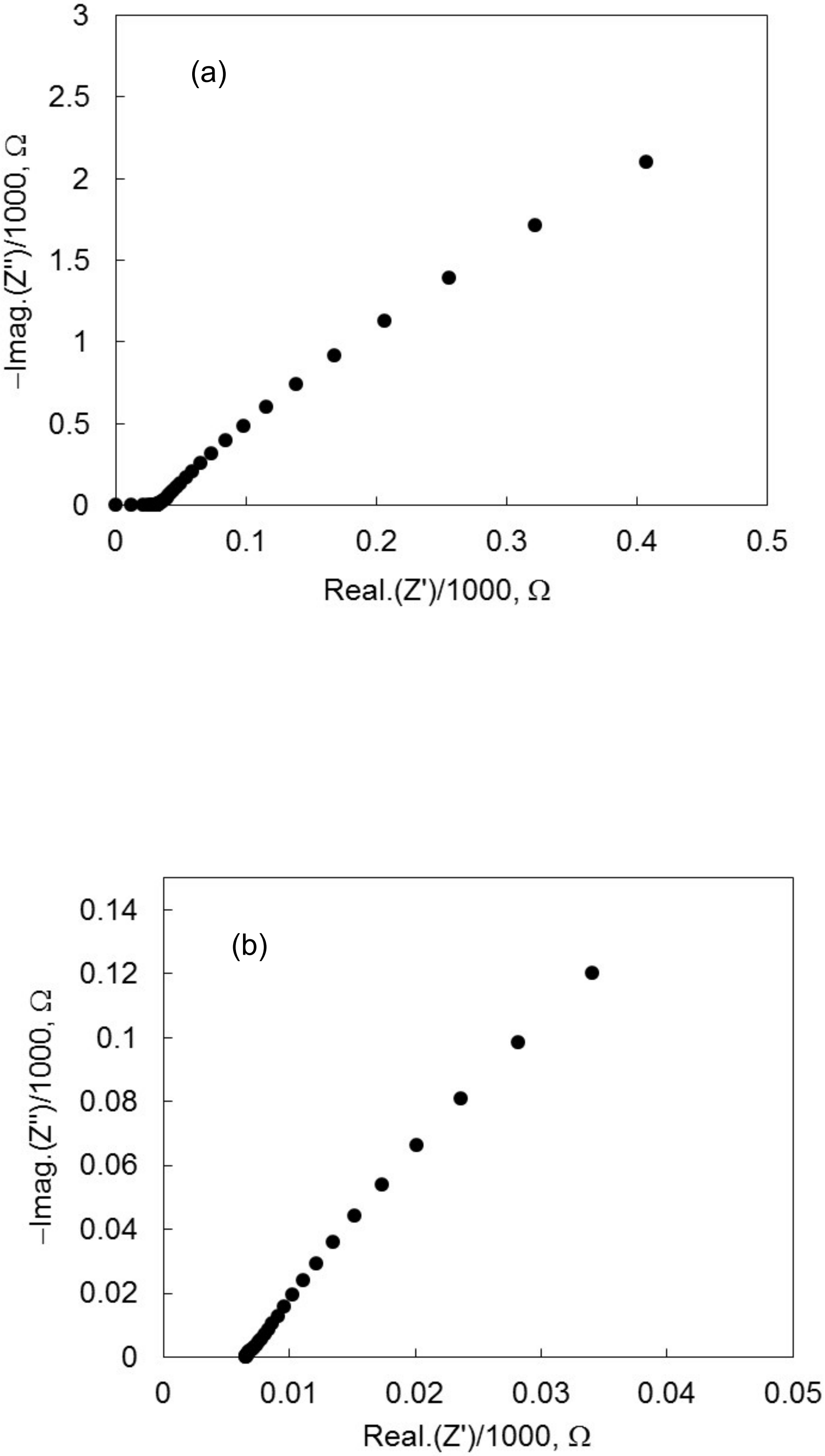

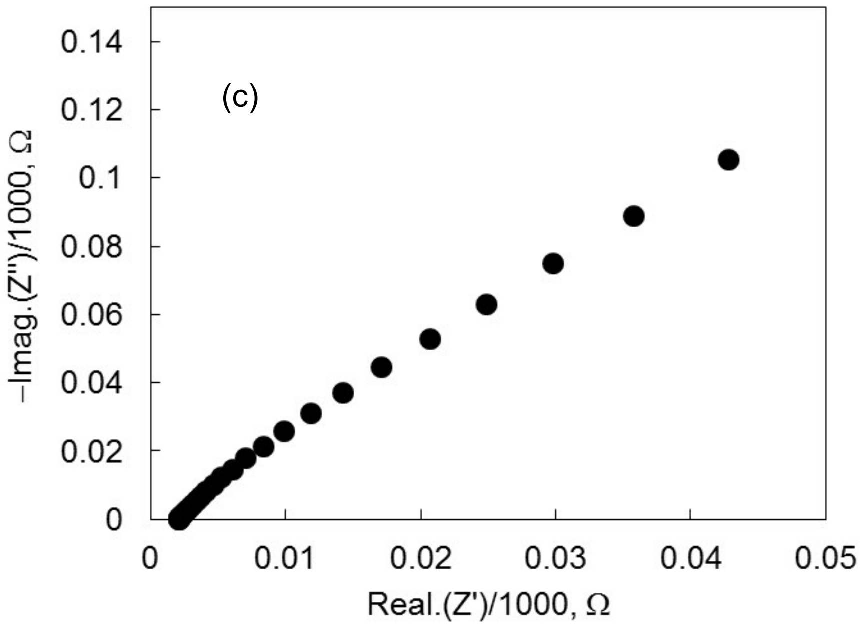
(c)
0.14
0.12
0.1
0.08
0.06
0.04
0.02
0
−Imag.(Z'')/1000, Ω
0
0.01
0.02
0.03
0.04
0.05
Real.(Z')/1000, Ω

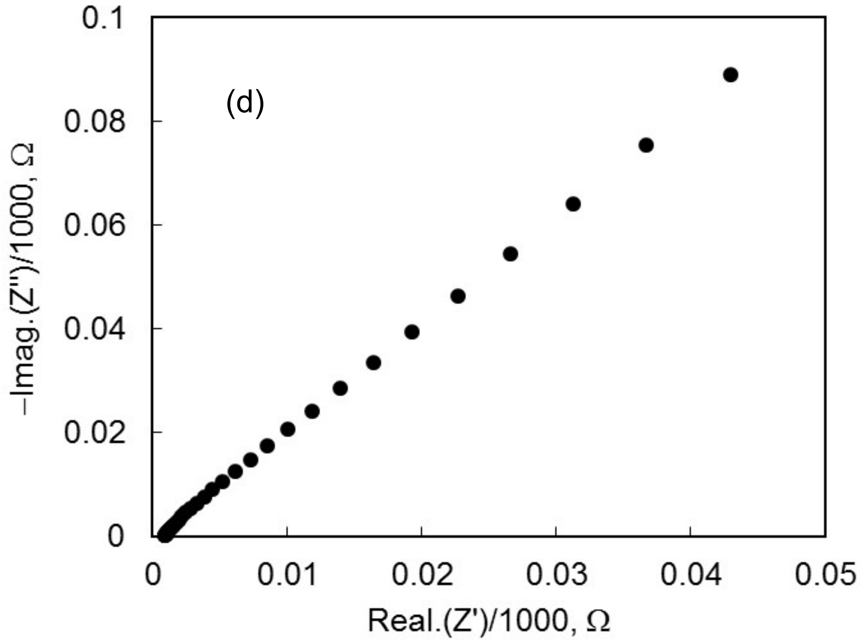
(d)
0.1
0.08
0.06
0.04
0.02
0
−Imag.(Z'')/1000, Ω
0
0.01
0.02
0.03
0.04
0.05
Real.(Z')/1000, Ω

Fig. S13. DSC thermograms (heating steps) of poly(ECH-MeIm$^+$Cl$^-$) ($M_{n(calc)}$ = 18 900, DP = 108), poly(ECH-MeIm$^+$TFSI$^-$) ($M_{n(calc)}$ = 45 400, DP = 108) and the equimolar mixture of the two (determined under N_2, 10 °C/min for each step).

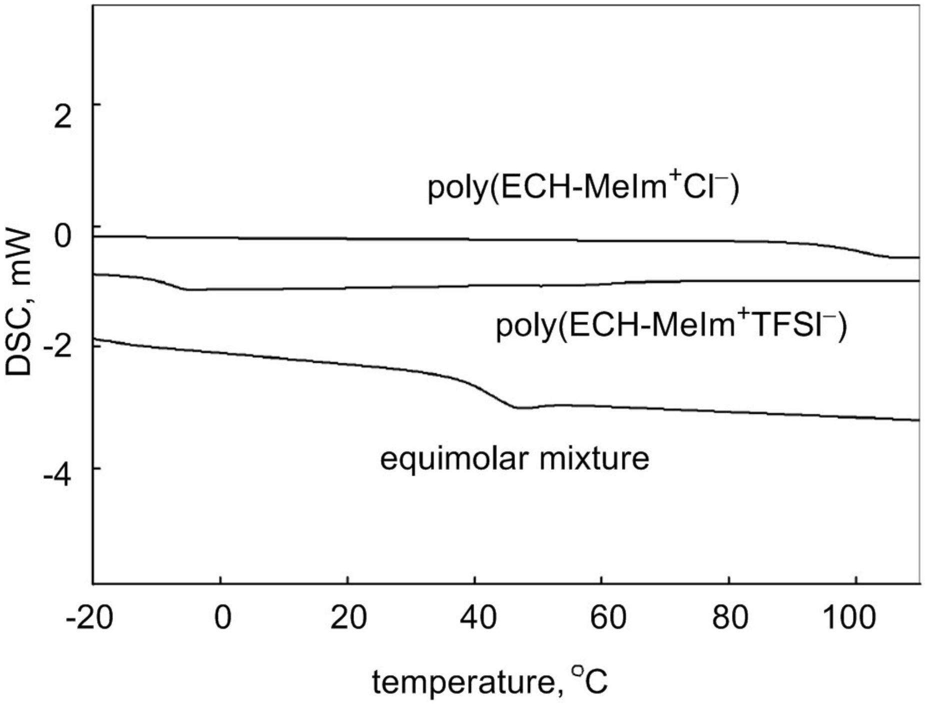

Table S2. Solubility of poly(ECH-MeIm$^+$Cl$^-$) ($M_{n(calc)}$ = 18 900, DP = 108), poly(ECH-MeIm$^+$TFSI$^-$)($M_{n(calc)}$ = 45 400, DP = 108), and the equimolar mixture of them.

	n-hexane	toluene	$CHCl_3$	THF	DMF	CH_3CN	acetone	MeOH	H_2O	DMSO
poly(ECH-MeIm$^+$Cl$^-$)	×	×	×	×	×	×	×	soluble	soluble	soluble
poly(ECH-MeIm$^+$TFSI$^-$)	×	×	×	soluble	soluble	soluble	soluble	×	×	soluble
equimolar mixture	×	×	×	×	×	soluble	soluble	soluble	×	soluble